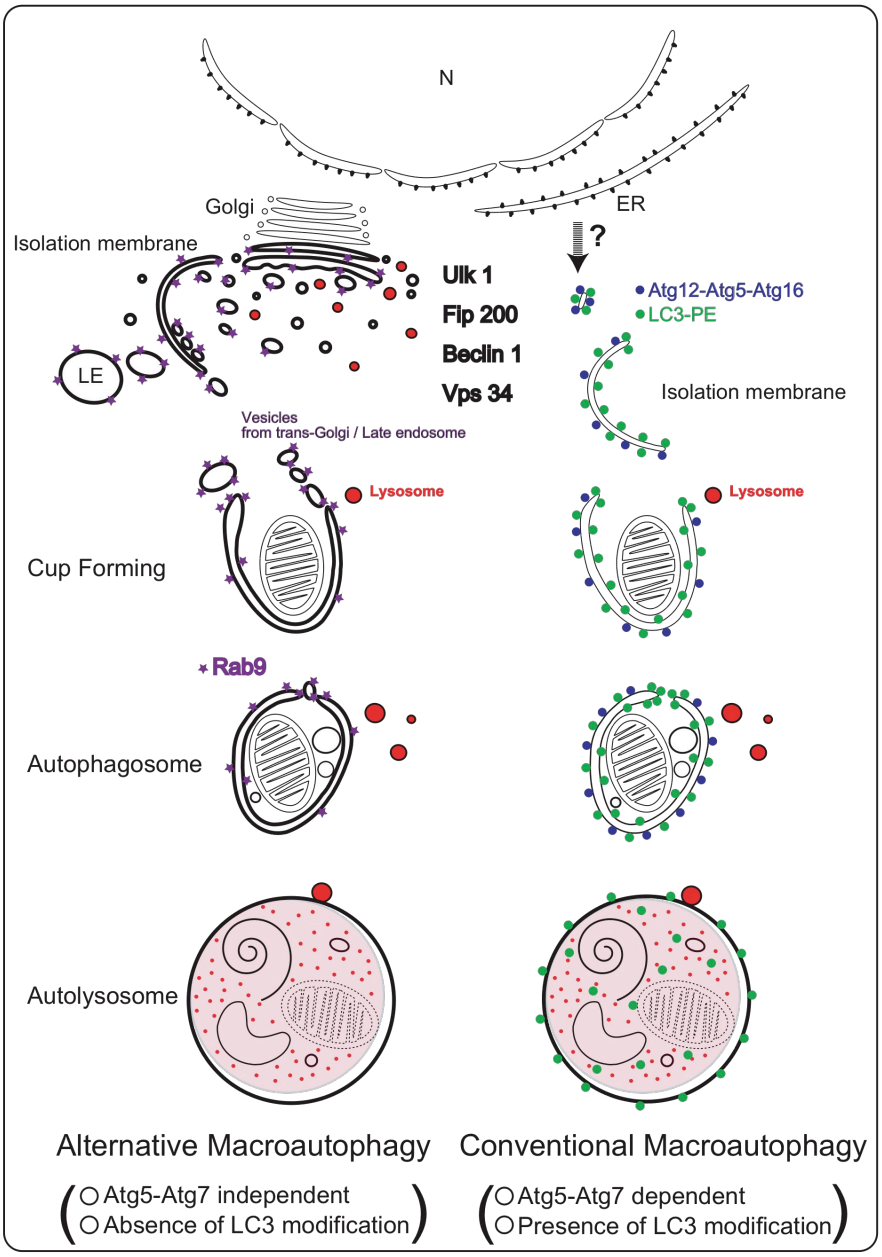


**Supplementary Figure 1. Hypothetical model of macroautophagy.** There are at least two modes of macroautophagy, *i.e.* conventional and alternative macroautophagy. Conventional macroautophagy depends on Atg5 and Atg7, is associated with LC3 modification and may originate from ER membrane. In contrast, alternative macroautophagy occurs independent of Atg5 or Atg7 expression and LC3 modification. The generation of autophagic vacuoles in this type of macroautophagy might be mediated by the fusion of isolation membranes with vesicles derived from the trans-Golgi and late endosomes (LE) in a Rab9-dependent manner. Although both these processes lead to bulk degradation of damaged proteins or organelles by generating autolysosomes, they seem to be activated by different stimuli, in different cell types and have different physiological roles.

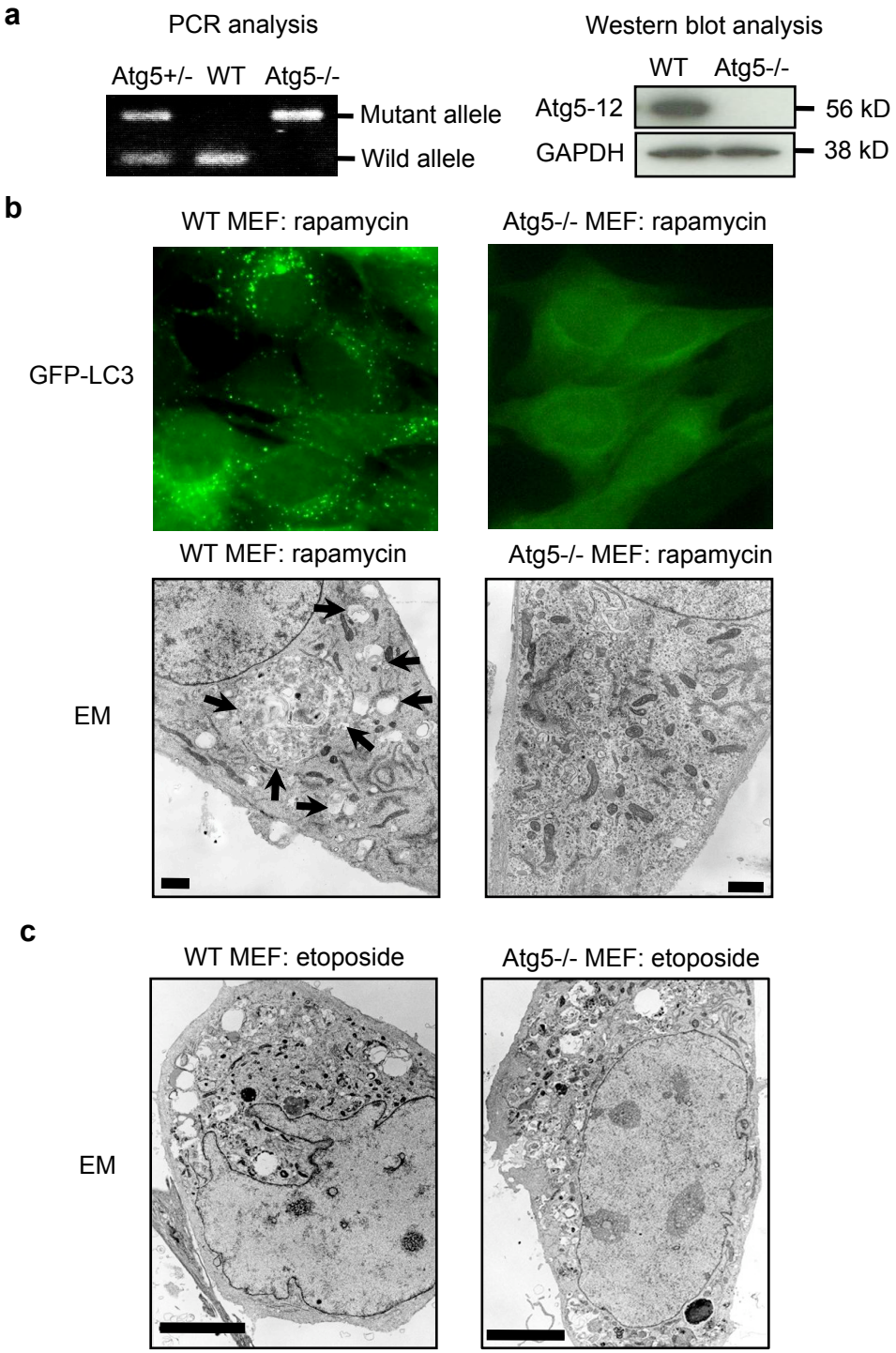


**Supplementary Figure 2. Induction of macroautophagy in Atg5-/- MEFs by etoposide, but not rapamycin.** **(a)** (left) PCR analysis of genomic DNA from Atg5+/−, wild type (WT) and Atg5−/−MEFs. (right) Immunoblot analysis of Atg5 in lysates from WT and Atg5−/− MEFs; GAPDH was a loading control. Anti-Atg5 (A0731) polyclonal antibody was purchased from Sigma-Aldrich. (**b**) WT and Atg5−/− MEFs were stably transfected with GFP-LC3, treated with 1 $\mu$M rapamycin for 18 hr and analysed by fluorescence micrograph and EM. In EM, arrows indicate autophagic vacuoles. Bar = 1 $\mu$m. (**c**) Electron micrograph of WT and Atg5−/− MEFs treated with etoposide (10 $\mu$M) for 18 hr, bar = 5 $\mu$m.

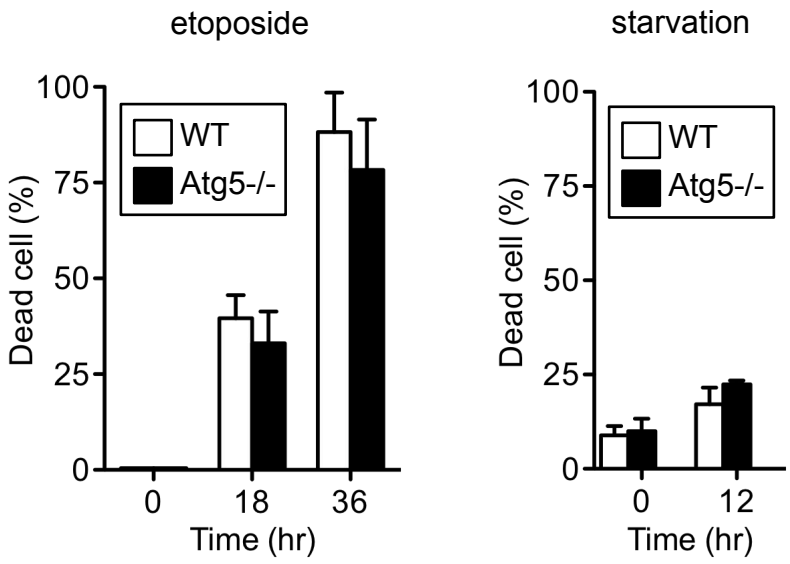


**Supplementary Figure 3. Similar viability of WT and Atg5–/– MEFs after treatment with etoposide and starvation.** WT and Atg5–/– MEFs were treated with 10 $\mu$M etoposide or starvation. Cell viability was measured by Annexin-V staining. Data are shown as the mean + s.d. (n = 4). The starved cells were cultured in Hanks' balanced salt solution supplemented with 1 mM sodium pyruvate, 10 mM Hepes/$Na^+$ (pH 7.4) and 0.05 mM 2-mercaptoethanol.

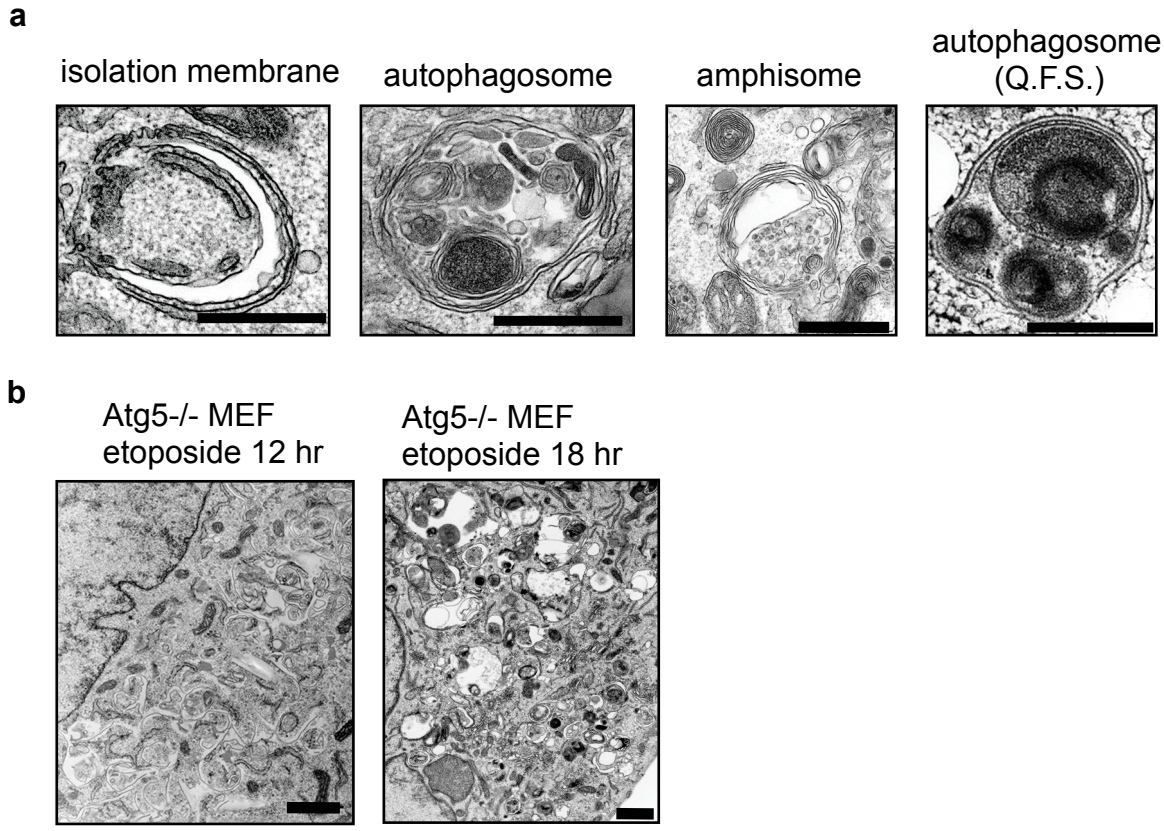


**Supplementary Figure 4. Typical autophagic structures in Atg5–/– MEFs treated by etoposide. (a)** Various autophagic structures in Atg5-/- MEFs treated by etoposide for 18 hr. Double membranous structure (isolation membrane), autophagosome containing organelles, amphisome (pre-autolysosome containing both autophagic and endocytic material), autophagosome obtained after quick-freezing followed by the freeze-substitution (Q.F.S.) technique. Bar = 0.5 $\mu$m. **(b)** Typical autophagic structures in Atg5–/–MEFs treated by etoposide for 12 and 18 hr. There were numerous double-membrane structures and few autolysosomes in Atg5–/– MEFs treated for 12 hr, whereas the situation was reversed at 18 hr, bar = 1 $\mu$m.

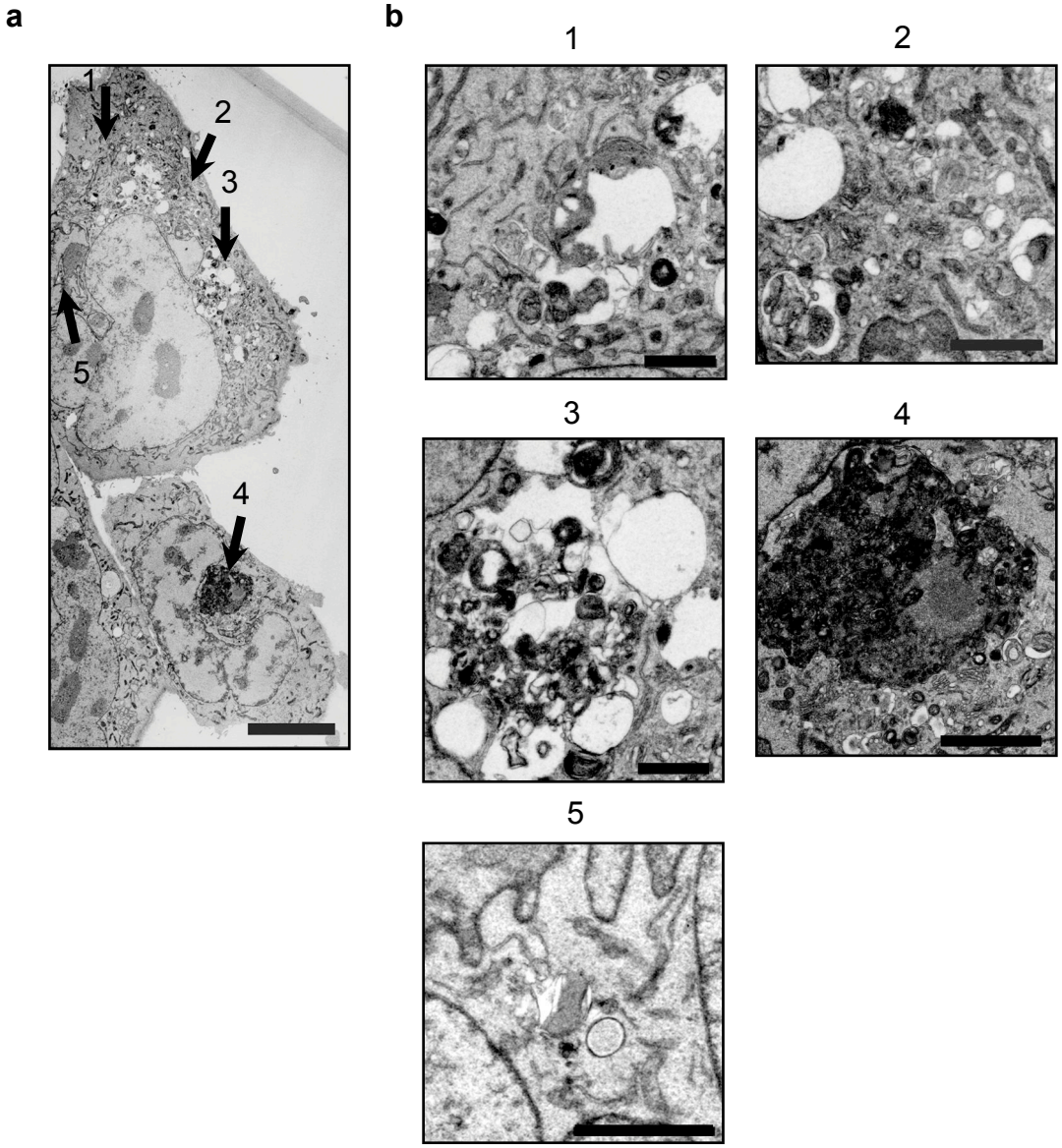


**Supplementary Figure 5. Magnified images of the etoposide-treated Atg5–/– MEFs immunostained by Lamp2 that were shown in Fig. 1a**. **(a)** Electron micrograph of the same Atg5–/– MEFs shown in Fig. 1a. Arrows indicate structures with punctate Lamp2 immunofluorescence. Bar = 10 $\mu$m. **(b)** Magnified images of structures with punctate Lamp2 fluorescence shown in **a**. Bar = 2.5 $\mu$m.

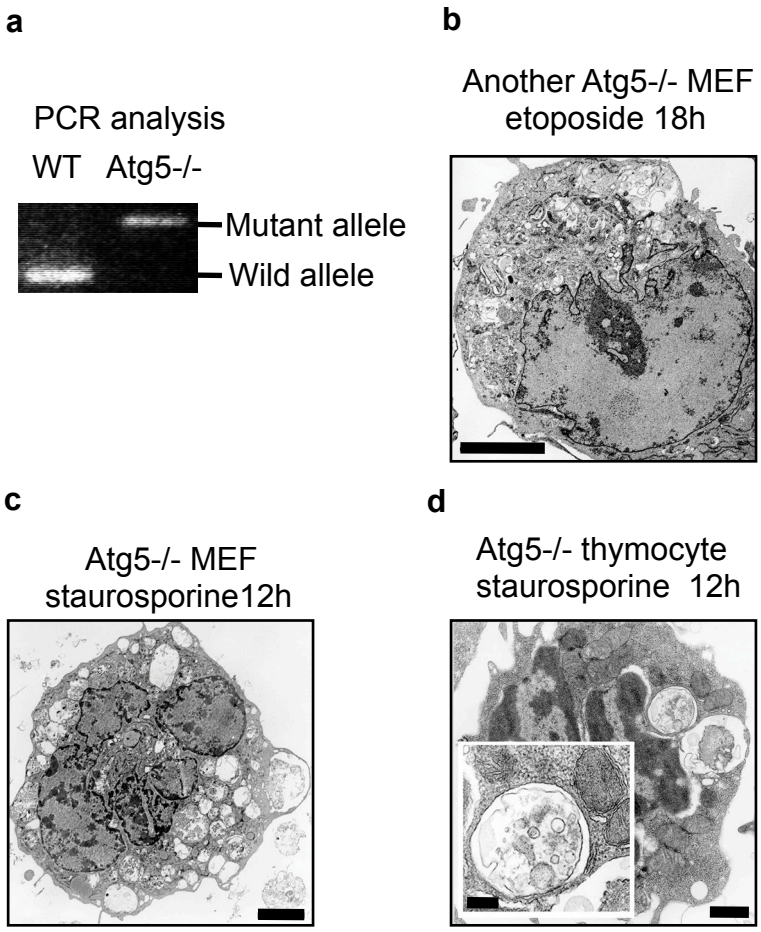


**Supplementary Figure 6. Induction of alternative macroautophagy in MEFs and thymocytes by etoposide and staurosporine.** (**a**) PCR analysis of genomic DNA from WT and Atg5−/− MEFs obtained from different mice. **(b)** Electron micrograph of other Atg5−/− MEFs treated with 10 $\mu$M etoposide for 18 hr, bar = 5 $\mu$m. Numerous autophagic vacuoles can be seen. (**c, d**) Electron micrograph of Atg5−/− MEFs (c) and Atg5−/− thymocytes (d) treated with 1 $\mu$M staurosporine for 12 hr. In (c), bar = 5 $\mu$m. (d) Thymocytes were harvested from an Atg5−/− embryo (E18.5). Bar = 0.5 $\mu$m. A magnified image of an autophagosome is shown in the inset. Bar = 0.2 $\mu$m.

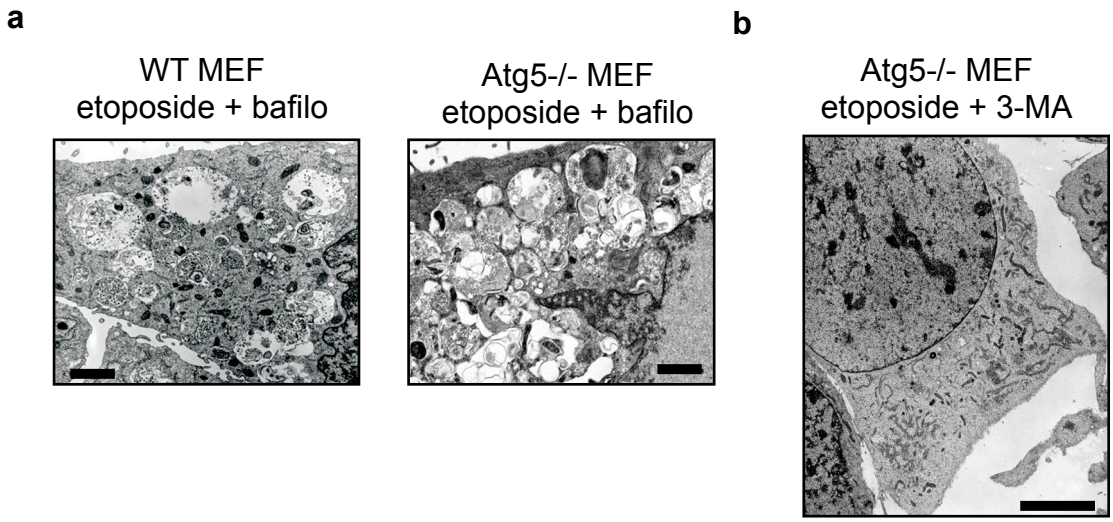


**Supplementary Figure 7. Representative electron micrographs of etoposide-treated MEFs in the presence of bafilomycin A1 and 3-MA.** **(a)** Accumulation of autophagosomes caused by bafilomycin A1 in MEFs treated with etoposide. WT and Atg5−/− MEFs were exposed to 10 $\mu$M etoposide in the presence of 10 nM bafilomycin A1 (bafilo) for 18 hr. Bar = 1 $\mu$m. **(b)** Suppression of autophagosome formation by 3-MA in Atg5−/− MEFs treated with etoposide. Atg5−/− MEFs were treated with etoposide (10 $\mu$M) in the presence of 5 mM 3-MA for 18 hr and EM was performed. Bar = 5 $\mu$m.

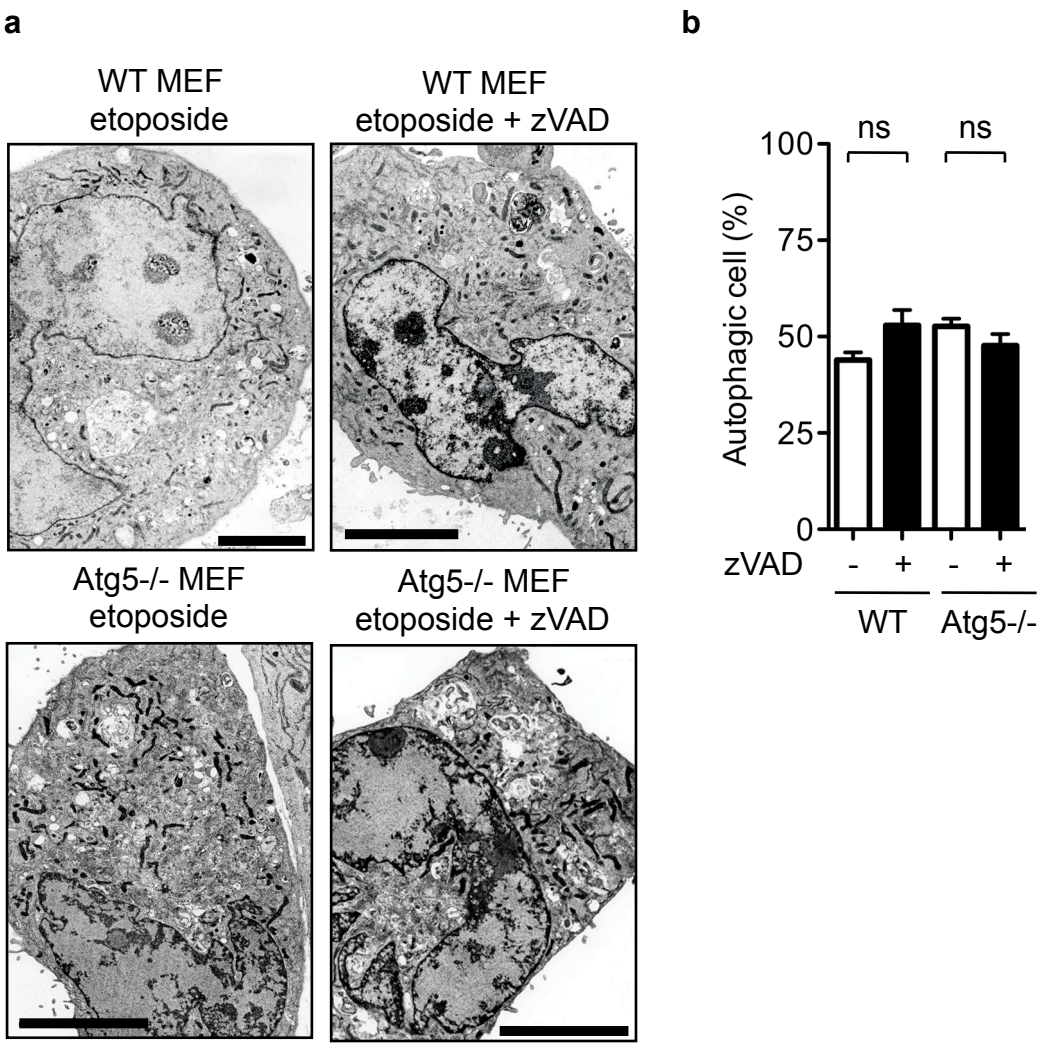


**Supplementary Figure 8. No effect of zVAD-fmk on etoposide-induced macroautophagy**. **(a)** Wild type (WT) and Atg5−/−MEFs were treated with 10 $\mu$M etoposide for 18 hr in the presence or absence of zVAD-fmk (100 $\mu$M). A representative photo is shown. Bar = 5 $\mu$m. **(b)** The percentage of autophagic cells (cells with punctate Lamp2 immunofluorescence) was calculated. Data are shown as the mean + s.d. (n = 4).

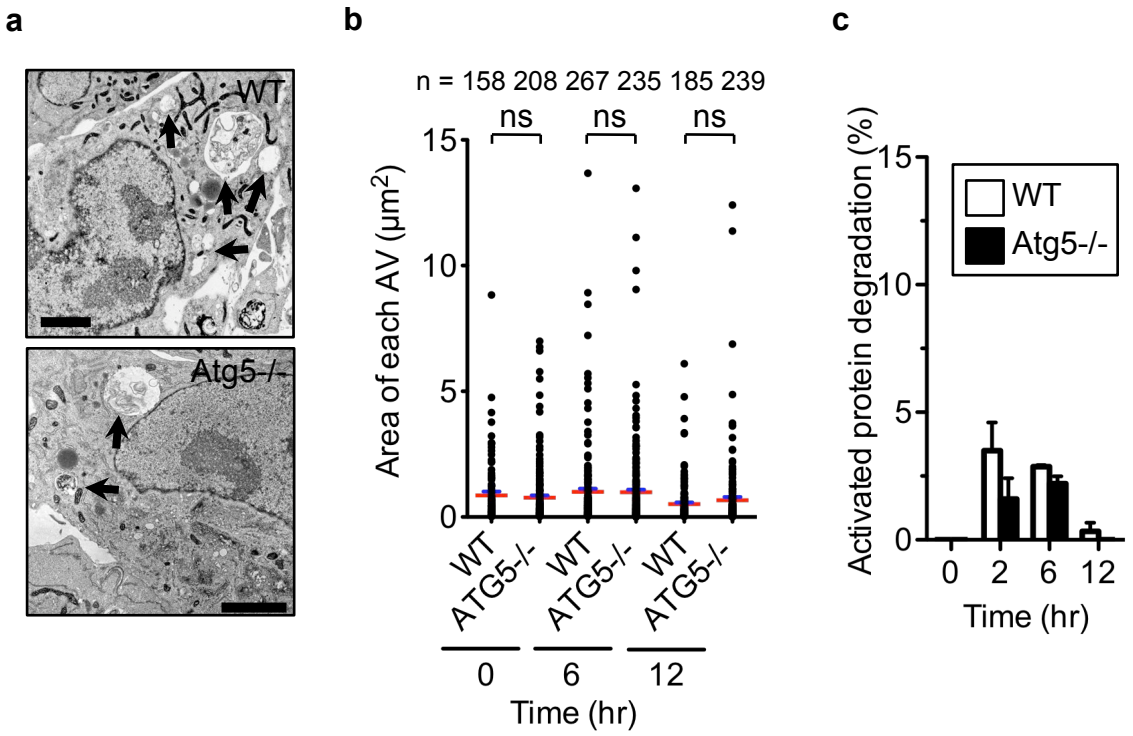


**Supplementary Figure 9. Induction of macroautophagy in Atg5–/– MEFs by starvation.** (**a**) Electron micrograph of WT and Atg5–/– MEFs starved for 6 hr. Arrows indicate autophagic vacuoles. Bar = 2.5 $\mu$m. (**b**) Size of each autophagic vacuole (AV) in starved MEFs. WT and Atg5–/– MEFs were starved for the indicated times, and the area of each autophagic vacuole was calculated (n = 20 cells each). The total number of autophagic vacuoles (n) is shown above the graph. Red and blue lines indicate the mean and s.e.m., respectively. 'ns' indicates no significant difference. (**c**) Induction of long-lived protein degradation by starvation. MEFs were starved for the indicated times in the presence of 100 $\mu$M zVAD-fmk, and the turnover of long-lived proteins was measured. Data are shown as the mean + s.d. (n = 4).

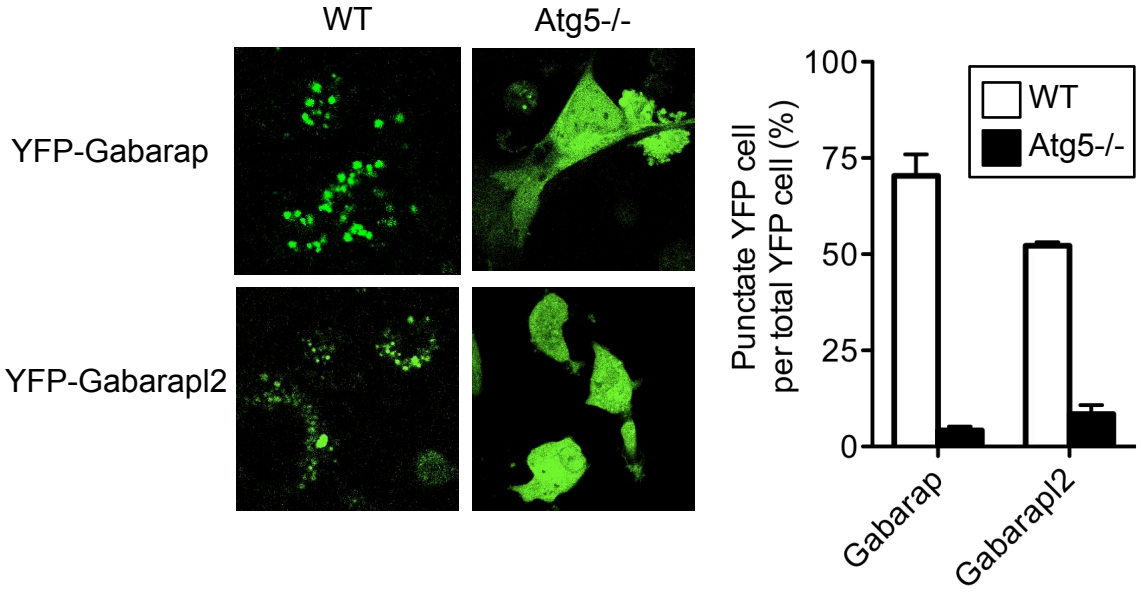


**Supplementary Figure 10. Punctate YFP-Gabarap and YFP- Gabarapl2 fluorescence in etoposide-treated WT MEFs but not Atg5–/– MEFs.** The same experiments as shown in Figs. 2b and c were performed by transiently expressing YFP-Gabarap and YFP-Gabarapl2, instead of stably expressing GFP-LC3, with etoposide treatment for 18 hr. (left) Representative photographs of WT and Atg5–/– MEFs were shown. (right) The percentage of MEFs with punctate YFP fluorescence was calculated relative to all YFP-expressing cells. Data are the mean + s.d. (n = 4).

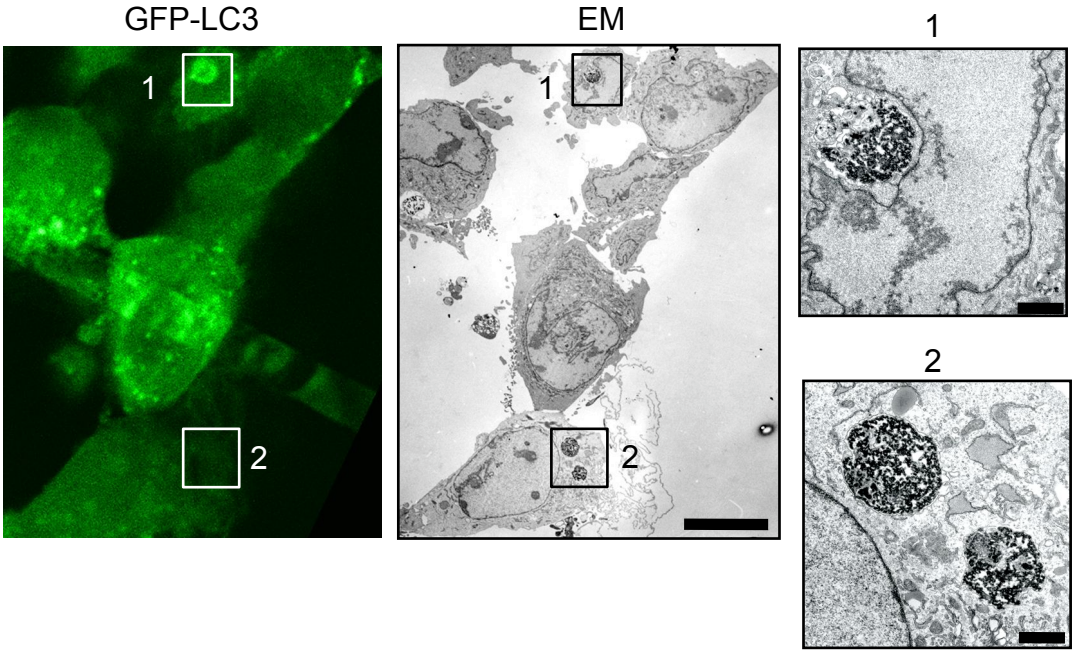


**Supplementary Figure 11. Induction of both conventional and alternative macroautophagy in etoposide-treated WT MEFs.** WT MEFs were stably transfected with GFP-LC3, cultured on coverslips, treated with 10 $\mu$M etoposide for 18 hr and fixed with glutaraldehyde and paraformaldehyde. After observing GFP-LC3 fluorescence (GFP-LC3), the same cells were fixed with $OsO_4$ and examined by EM (EM). Bar = 10 $\mu$m. Magnified photo is the area indicated by the squares in 'GFP-LC3' and 'EM'. Bar = 1 $\mu$m. Both GFP-LC3-positive (conventional) macroautophagy (photo 1) and GFP-LC3-negative (alternative) macroautophagy (photo 2) were activated in etoposide-treated WT MEFs.

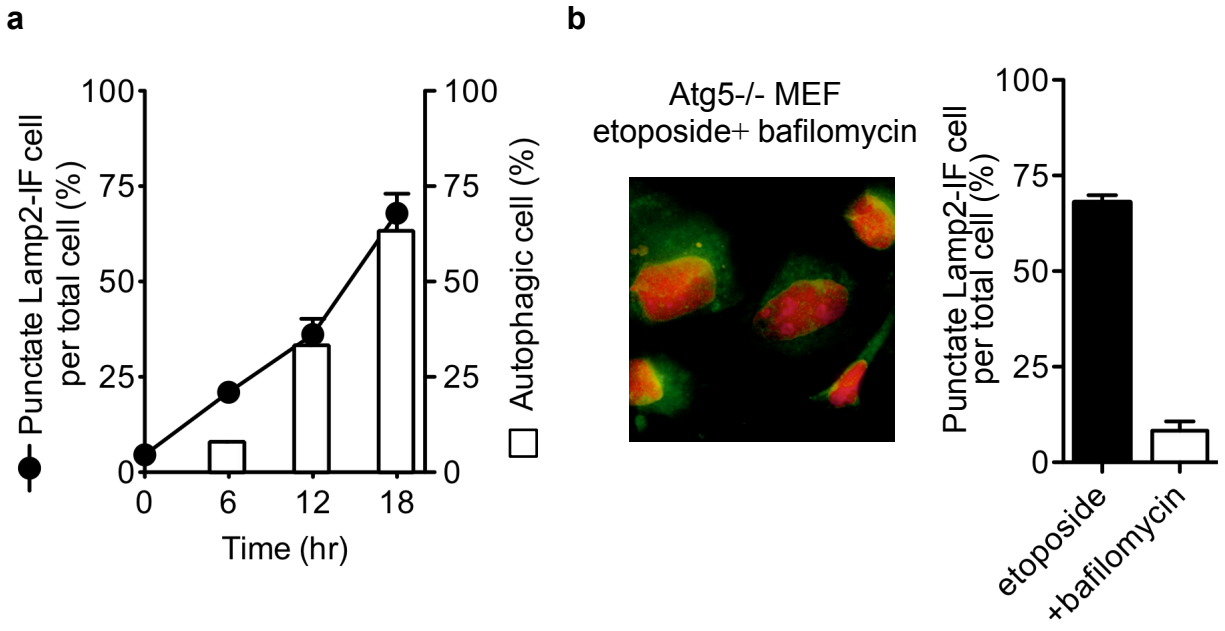


**Supplementary Figure 12. Detection of alternative macroautophagy by Lamp2 immunostaining. (a)** Atg5−/−MEFs were treated with 10 $\mu$M etoposide. Then, MEFs were examined by Lamp2 immunofluorescence and by EM. The percentage of cells with punctate Lamp2 immunostaining was calculated (filled circles). The percentage of autophagic cells was also analysed by EM (open bars). Autophagic cells were defined as cells in which autophagic vacuoles exceeded 6% of the total cytoplasmic area, which was the upper limit in untreated healthy cells. Data are the mean ± s.d. (n = 4). **(b)** Inhibition of punctate Lamp2 immunofluorescence by bafilomycin A1 in etoposide-treated Atg5−/− MEFs. Cells were treated with 10 $\mu$M etoposide in the presence of 10 nM bafilomycin A1 for 18 hr. A representative photograph (left) and the percentage of cells with punctate Lamp2 immunofluorescence (right) are shown. Data are the mean ± s.d. (n = 4).

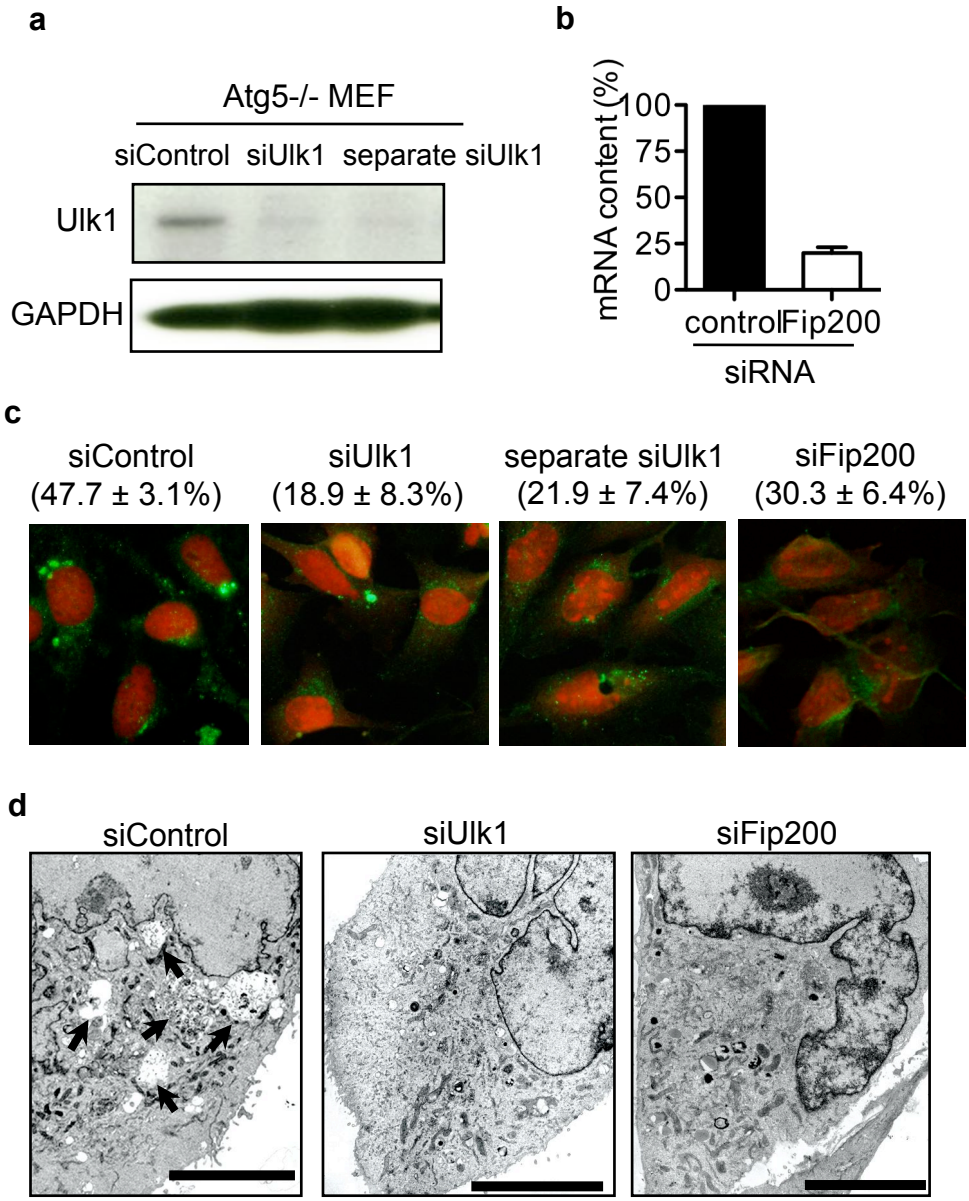


**Supplementary Figure 13. Involvement of Ulk1 and Fip200 in alternative macroautophagy of Atg5–/– MEFs. (a, b)** Atg5–/– MEFs were transiently transfected with 10 $\mu$g of two Ulk1 siRNAs, Fip200 siRNA or the negative control (siControl) for 24 hr. (a) Expression of Ulk1 and GAPDH (loading control) was assessed by Western blot analysis. (b) Expression of Fip200 was analysed by qPCR. Data are shown as the mean + s.d. (n = 3). **(c, d)** Inhibition of alternative macroautophagy in etoposide-treated Atg5–/– MEFs by siRNA for Ulk1 or Fip200. Atg5–/– MEFs were transfected with indicated siRNAs for 24 hr and treated with 10 $\mu$M etoposide for 18 hr. The cells were then examined for Lamp2 immunofluorescence (c) and by EM (d). In (c), representative photographs are shown. The percentage of cells with punctate Lamp2 immunostaining is shown as the mean ± s.d. (n = 4). In (d), representative photographs are shown, bar=5 $\mu$m.

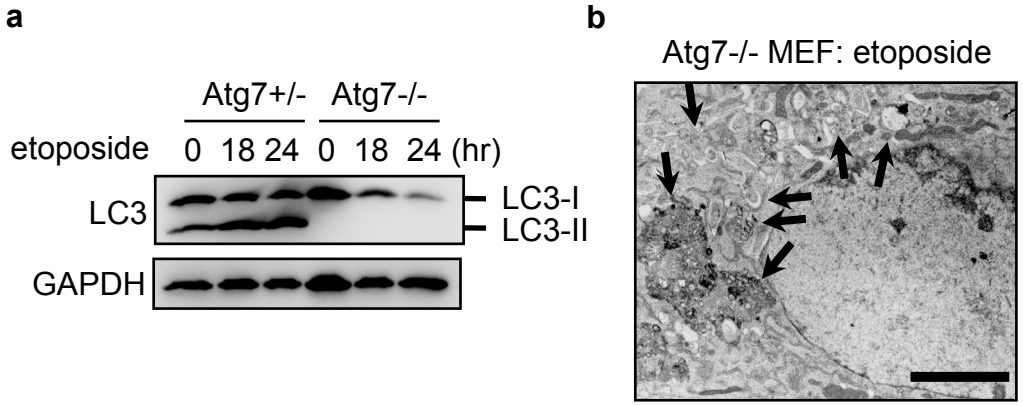


**Supplementary Figure 14. Induction of alternative macroautophagy in Atg7–/– MEFs by etoposide**. **(a)** Formation of LC3-II in etoposide-treated Atg7+/–MEFs but not Atg7–/– MEFs. Atg7+/– and Atg7–/– MEFs were treated with 10 $\mu$M etoposide for the indicated times. LC3-II production was assessed by Western blot analysis; GAPDH was a loading control. **(b)** Electron micrograph of Atg7–/– MEFs treated with etoposide (10 $\mu$M) for 18 hr. Arrows indicate autophagic vacuoles. Bar = 5 $\mu$m.

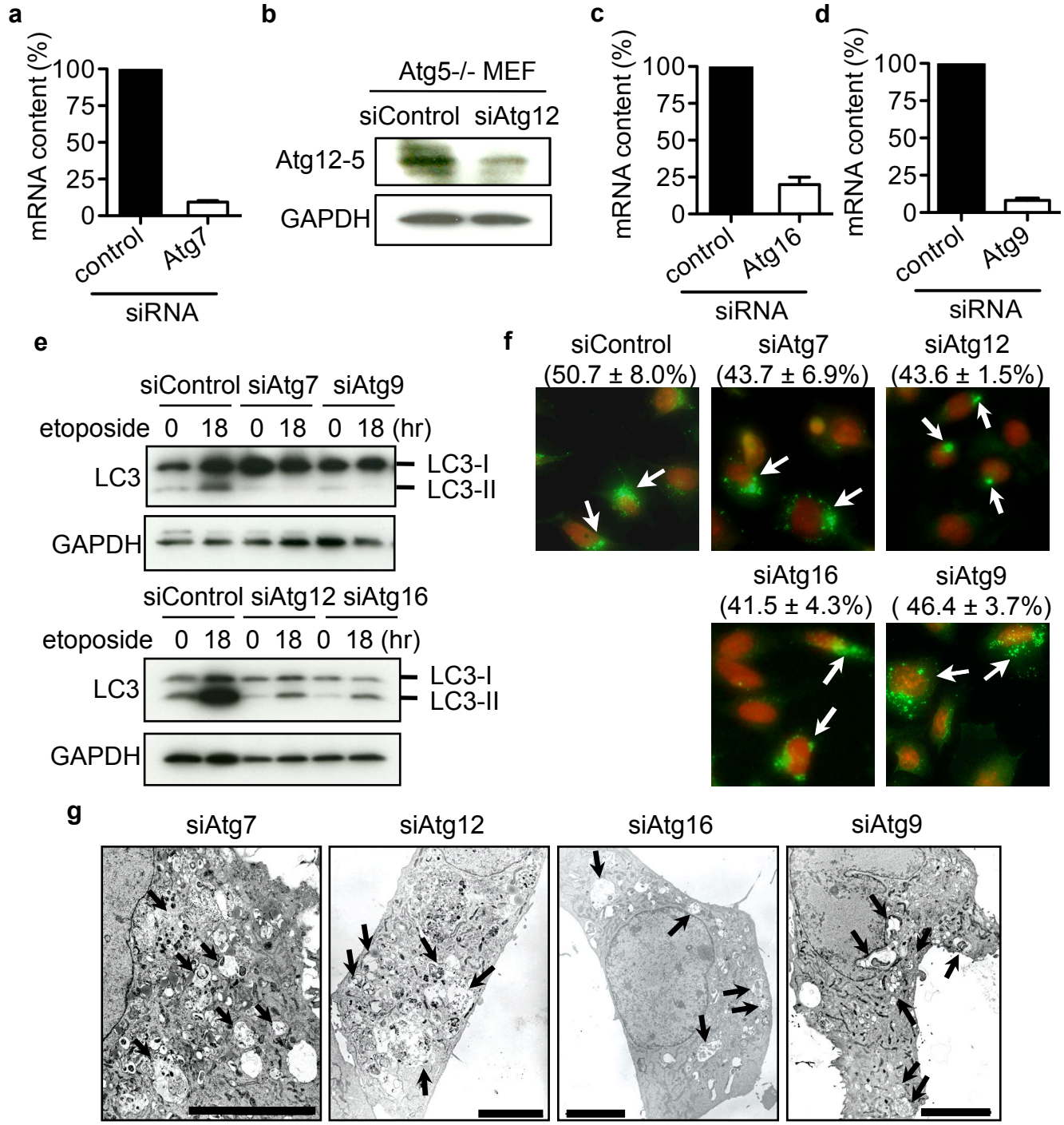


**Supplementary Figure 15. No involvement of Atg7, Atg12, Atg16 or Atg9 in alternative macroautophagy of Atg5–/– MEFs.** Atg5–/–MEFs (a-d, f,g) and WT MEFs (e) were transiently transfected with indicated siRNAs (10 $\mu$g) for 24 hr. (a-d) Expression of proteins was analysed by qPCR and by immunoblot. Data are shown as the mean + s.d. (n = 4). Anti-Atg12 polyclonal antibody was provided from Prof. Mizushima. (e) WT MEFs were then treated with 10 $\mu$M etoposide and examined for LC3 Western blotting. These siRNAs efficiently suppressed conventional macroautophagy. **(f, g)** Atg5–/– MEFs were then treated with 10 $\mu$M etoposide for 18 hr and examined for Lamp2 immunofluorescence (f) and by EM (g). In (f), the percentage of cells with punctate Lamp2 immunofluorescence is shown as the mean ± s.d. (n = 4). In (f, g), arrows indicate autophagic vacuoles. Bar = 5 $\mu$m.

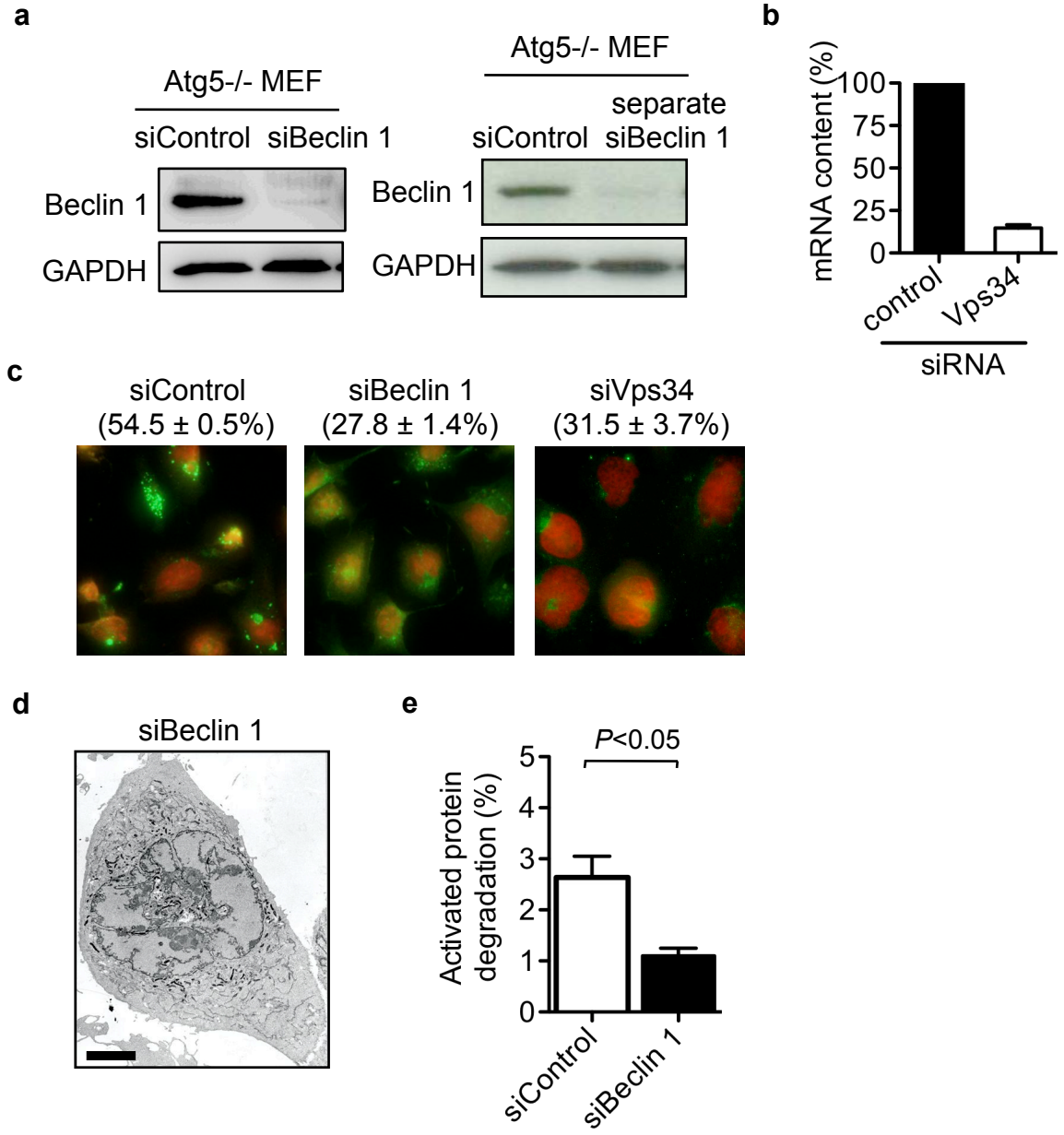


**Supplementary Figure 16. Involvement of Beclin 1 and Vps34 in alternative macroautophagy of Atg5–/– MEFs. (a, b)** Atg5–/– MEFs were transiently transfected with indicated siRNAs (10 $\mu$g) for 24 hr. (a) Expression of Beclin 1 and GAPDH (loading control) was assessed by Western blot analysis. Anti-Beclin 1 (Clone 20) monoclonal antibody was purchased from BD Biosciences. (b) Expression of Vps34 was analysed by qPCR. Data are shown as the mean + s.d. (n = 4). **(c, d)** Atg5–/– MEFs were transfected with indicated siRNAs for 24 hr and treated with 10 $\mu$M etoposide for 18 hr. The cells were then examined for Lamp2 immunofluorescence (c) and by EM (d). In (c), the percentage of cells with punctate Lamp2 immunostaining is shown as the mean ± s.d. (n = 4). In (d), bar=5 $\mu$m. (e) Atg5-/- MEFs were treated with indicated siRNAs (10 $\mu$g), followed by exposure to 10 $\mu$M etoposide in the presence of 100 $\mu$M zVAD-fmk for 12 h. The turnover of long-lived protein was then measured. Data are the mean + s.d. (n = 4).

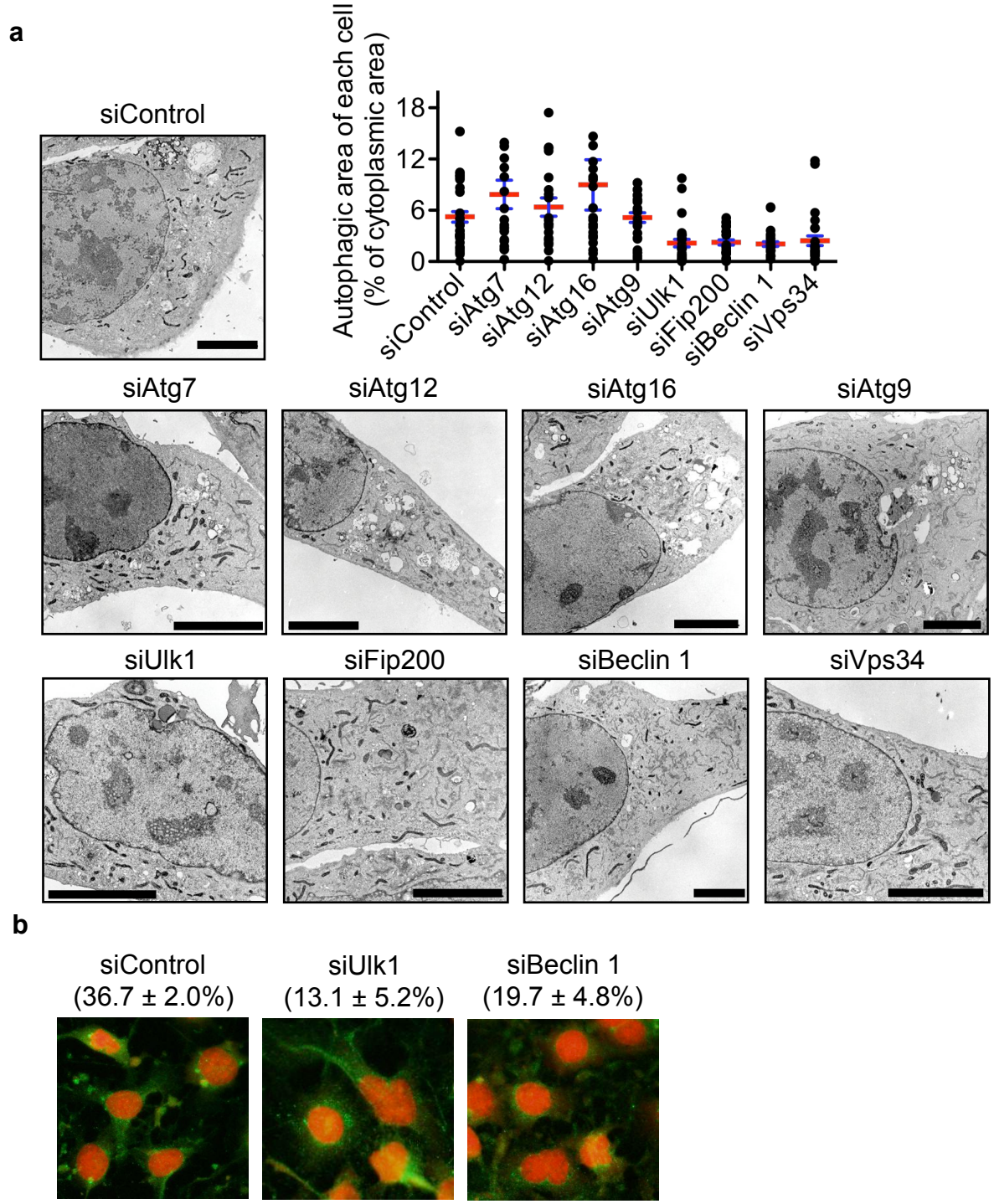


**Supplementary Figure 17. Involvement of Ulk1, Fip200, Beclin 1 and Vps34, but not Atg7, Atg12, Atg16 or Atg9, in alternative macroautophagy induced by starvation and staurosporine.** Atg5−/− MEFs were transiently transfected with 10 $\mu$g of the indicated siRNAs for 24 hr. **(a)** The cells were then starved for 6 hr and analysed by EM, bar=5 $\mu$m. The autophagic area per cell was calculated (n= 20 cells each). Red and blue lines indicate the mean and s.e.m., respectively. **(b)** The cells were then treated with 1 $\mu$M staurosporine for 12 hr and examined for Lamp2 immunofluorescence. The percentage of cells with punctate Lamp2 immunostaining is shown as the mean ± s.d. (n = 3).

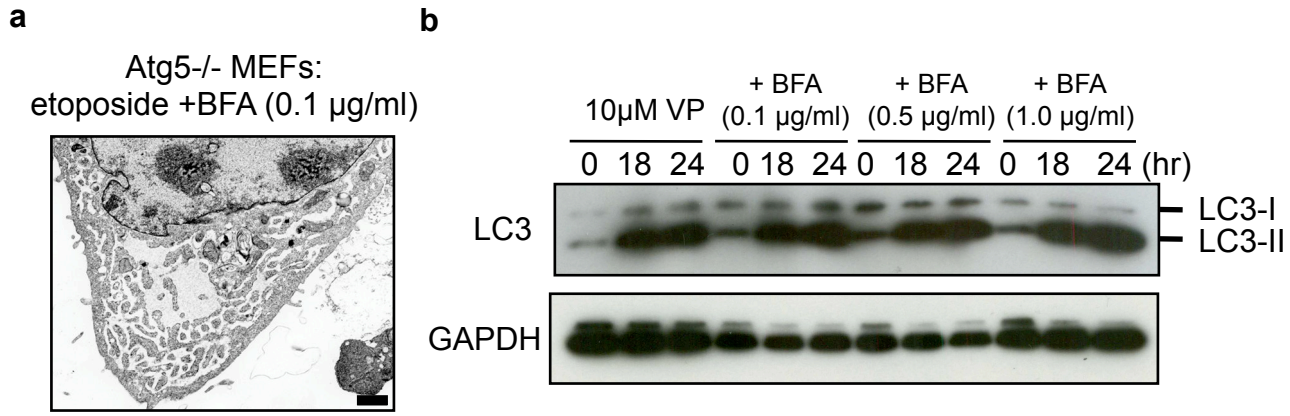


**Supplementary Figure 18. Inhibition of alternative, but not conventional, macroautophagy by brefeldin A. (a)** Atg5−/− MEFs were treated with 10 $\mu$M etoposide for 18 hr in the presence of brefeldin A (BFA, 0.1 $\mu$g/ml). Bar = 1 $\mu$m. The ER was highly dilated under this condition. Most Golgi stacks had disappeared completely and macroautophagy was largely suppressed. **(b)** There was no effect of LC3 autophagic modification by BFA in etoposide-treated WT MEFs.

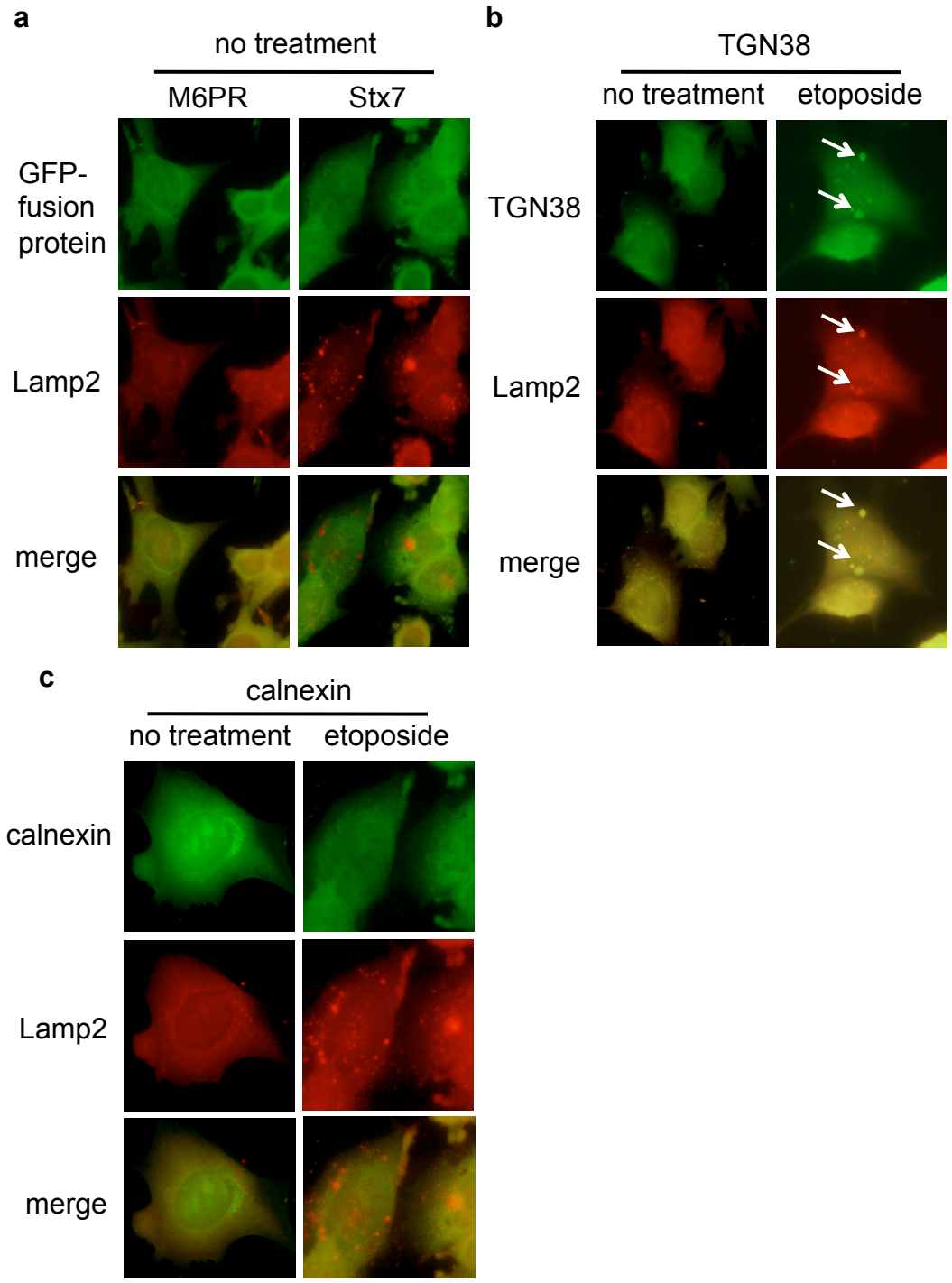


**Supplementary Figure 19. Involvement of trans-Golgi/endosomes, but not ER, in alternative macroautophagy.** (**a**) Atg5−/−MEFs were transiently transfected with organelle markers [M6PR-GFP (trans-Golgi and late endosomes) and GFP-Stx7 (late endosomes)] for 24 hr. The cells were then fixed and co-stained with Lamp2 antibody. Fluorescence images of the organelle markers and Lamp2 are merged in the bottom panel. M6PR-GFP and GFP-Stx7 were not co-localised with Lamp2 in healthy cells. **(b, c)** Redistribution of TGN38, but not calnexin, into Lamp2-positive vacuoles by etoposide. Atg5−/− MEFs were treated with or without etoposide for 18 hr. The cells were then fixed and immunostained with anti-TGN38 (green), anti-calnexin (green) and anti-Lamp2 (red) antibodies. Fluorescence images are merged in the bottom panel.

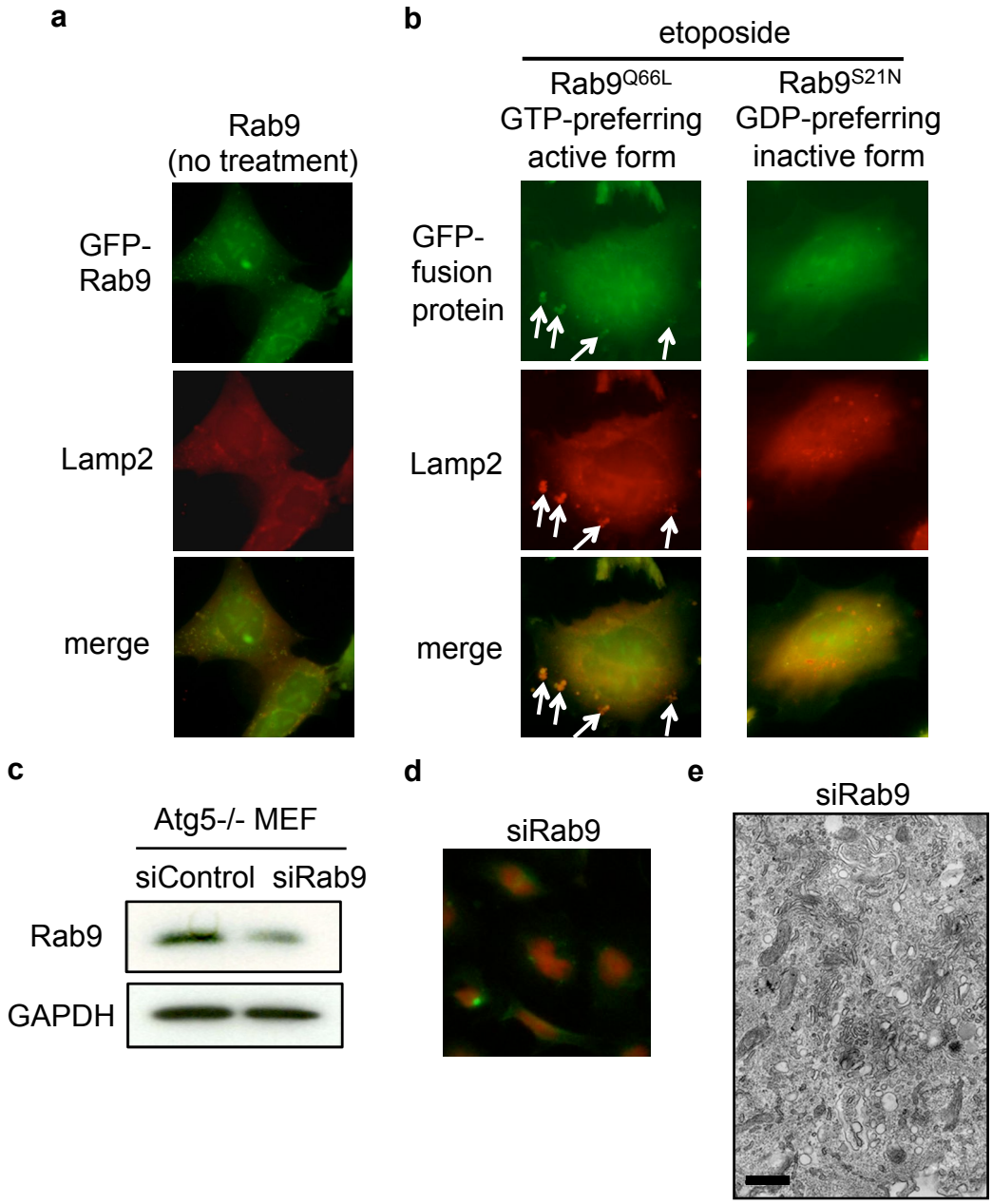


**Supplementary Figure 20. Effect of Rab9 on alternative macroautophagy.** (**a**) Atg5–/–MEFs were transiently transfected with GFP-Rab9 for 24 hr. The cells were then fixed and co-stained with Lamp2 antibody. GFP-Rab9 was not co-localised with Lamp2 in healthy cells. **(b)** Similar experiments to those in Fig. 3f were performed using GFP-Rab9$^{Q66L}$ (GTP-preferring active form) and GFP-Rab9$^{S21N}$ (GDP-preferring inactive form). **(c-e)** Atg5–/– MEFs were transiently transfected with indicated siRNAs (10 $\mu$g) for 24 hr. (c) Expression of Rab9 was assessed by Western blot analysis. Anti-Rab9 (R5404) monoclonal antibody was purchased from Sigma-Aldrich. (d, e) The cells were then treated with 10 $\mu$M etoposide for 18 hr and examined for Lamp2 immunofluorescence (d) and by EM (e). In (e), bar=0.5 $\mu$m.

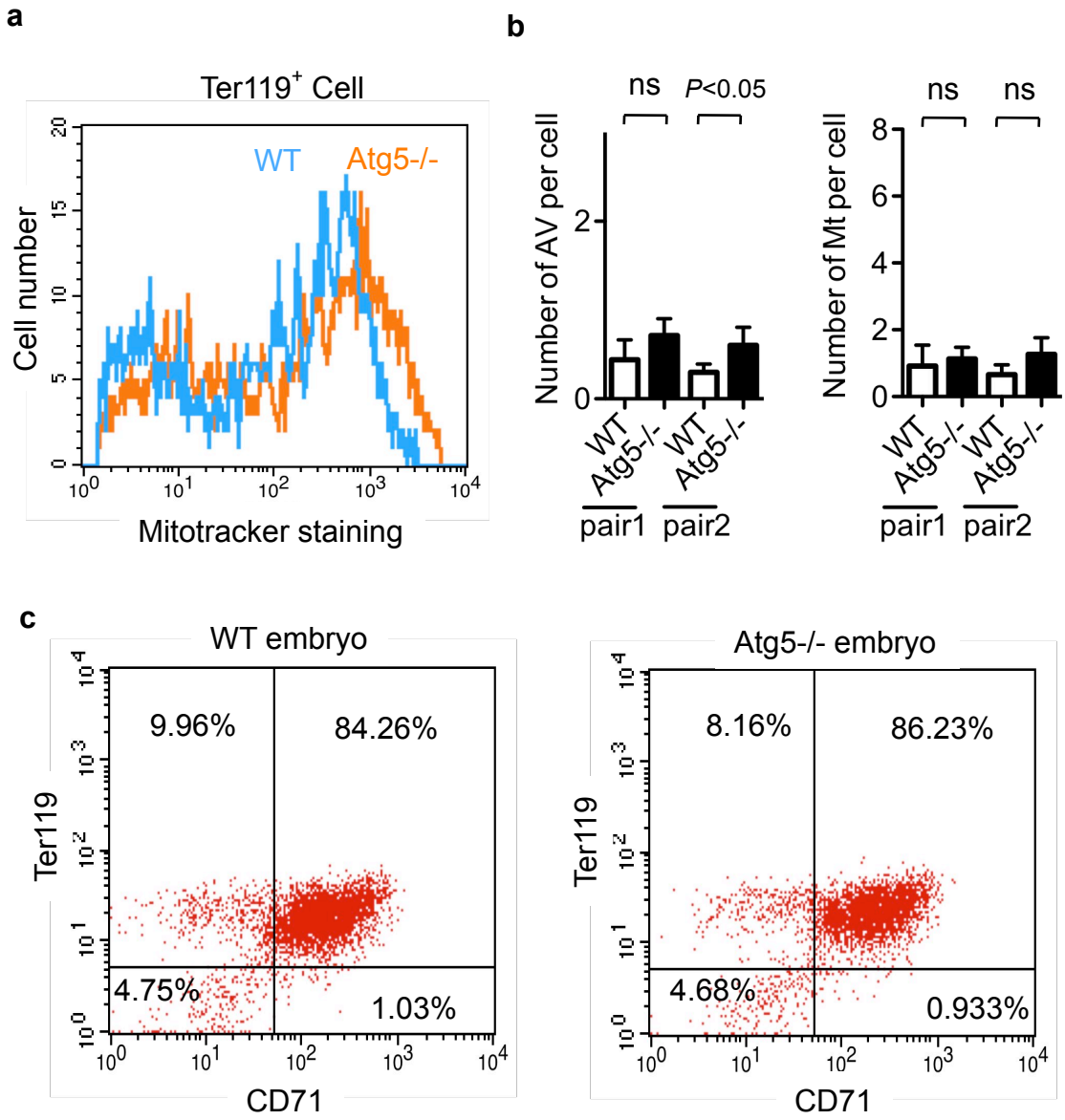


**Supplementary Figure 21. Normal clearance of mitochondria by macroautophagy in erythroid cells. (a)** Erythroid cells were recovered from the foetal liver (E14.5) and stained with Ter119 and mitotracker green. Mitochondrial content in Ter119$^+$ erythroid cells is shown. **(b)** The number of autophagic vacuoles (left) and persisting mitochondria (right) in erythrocytes was assessed by EM. The same experiments as shown in Figs. 4m and 4o were performed with different mice. Data are the mean + s.d. (n = 32). **(c)** Ter119 versus CD71 staining of erythroid cells from embryo (E16.5).